Acta Cryst
E
CRYSTALLOGRAPHIC COMMUNICATIONS

ISSN 2056-9890

Crystal structure of an ordered $[WOF_5]^-$ salt: (1,10-phen-H)$[WOF_5]$ (1,10-phen = 1,10-phenanthroline)

Douglas Turnbull and Michael Gerken*

Canadian Centre for Research in Advanced Fluorine Technologies, Department of Chemistry and Biochemistry, University of Lethbridge, 4401 University Drive West, Lethbridge, Alberta, Canada, T1K 3M4. *Correspondence e-mail: michael.gerken@uleth.ca

Received 9 July 2020
Accepted 16 July 2020

Edited by A. M. Chippindale, University of Reading, England

Keywords: tungsten; fluoride; oxide; crystal structure; O/F ordered anion.

CCDC reference: 2016898

Supporting information: this article has supporting information at journals.iucr.org/e

Crystals of 1,10-phenanthrolinium pentafluoridooxidotungstate(VI), (1,10-phen-H)$[WOF_5]$ (1,10-phen = 1,10-phenanthroline, $C_{12}H_8N_2$), were obtained upon hydrolysis of WF_6(1,10-phen) in CH_3CN at 193 K. The (1,10-phen-H)$[WOF_5]$ salt contains a rare example of a $[WOF_5]^-$ anion in which the oxygen and fluorine atoms are ordered. This ordering was verified by bond-valence determinations and structural comparisons with $[Xe_2F_{11}][WOF_5]$ and Lewis acid-base adducts of WOF_4 with main-group donor ligands. The crystal packing is controlled by N—H⋯F hydrogen bonding that is directed exclusively to the axial F atom as a result of its increased basicity caused by the *trans* influence of the oxido ligand.

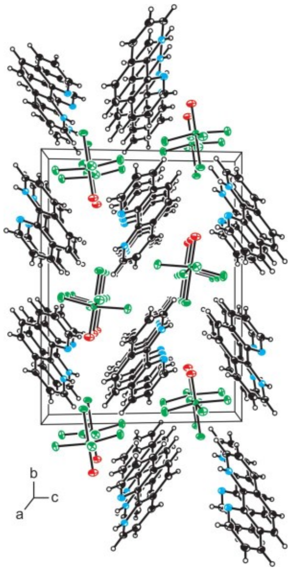

1. Chemical context

The crystal structure of tetrameric, fluorine-bridged WOF_4 (Edwards & Jones, 1968), as well as those of various fluoridooxidotungstates(VI) of the form $[WO_nF_{6-n}]^{n-}$ (n = 1–3), are characterized by extensive disorder between the oxido and fluorido ligands (Voit *et al.*, 2006). Such disorder complications originally led to the incorrect assumption that WOF_4 existed as an oxygen-bridged species. This was later disproved by vibrational spectroscopic studies of WOF_4 that revealed exclusively terminal W═O bonds (Bennett *et al.*, 1972; Asprey *et al.*, 1972). In $[WO_nF_{6-n}]^{n-}$ anions, the nature of the O/F disorder can be controlled by the properties of the countercations. For example, $Na[WO_2F_4]$ is ordered (Vlasse *et al.*, 1982; Chaminade *et al.*, 1986), whereas $Rb[WO_2F_4]$ (Udovenko & Laptash, 2008*a*) and $Cs[WO_2F_4]$ (Srivastava *et al.*, 1992) are statically disordered, and $[NH_4]_2[WO_2F_4]$ exhibits simultaneous static and dynamic disorder, both of which are quenched below 201 K to reveal an ordered structure (Udovenko & Laptash, 2008*b*). In addition, the double salt, $[HNC_6H_6OH]_2[Cu(NC_5H_5)_4][WO_2F_4]_2$, exhibits ordered $[WO_2F_4]^{2-}$ anions at 153 K as a result of H⋯F and Cu⋯O secondary-bonding interactions (Welk *et al.*, 2001). An ordered $[WO_3F_3]^{3-}$ fragment was identified within $Pb_5W_3O_9F_{10}$ (Abrahams *et al.*, 1987) and, despite extensive dynamic disorder within $[NH_4]_3[WO_3F_3]$ (Voit *et al.*, 2006), the stereochemistry could be resolved from the observed displacement of the tungsten atoms from their octahedral symmetry centres (Udovenko & Laptash, 2008*a*). In all cases, mutual *cis* arrangements of the oxido ligands are preferred (*i.e.*, *cis*-$[WO_2F_4]^{2-}$ and *fac*-$[WO_3F_3]^{3-}$). A *trans* influence from the oxido ligands results in increased electron density on

OPEN ACCESS

the effected fluorido ligands, and it is these fluorido ligands that participate in fluorine bridging within multinuclear systems, such as in WOF_4 and in various $[W_2O_2F_9]^-$ salts with different counterions {$[H_3O]^+$(Hoskins *et al.*, 1987); $[WF_4(2,2'\text{-bipy})_2]^{2+}$(Arnaudet *et al.*, 1992); $[Os_3(CO)_{12}H]^+$ (Crossman *et al.*, 1996); $[XeF_5]^+$(Bortolus *et al.*, 2020); Li–Cs^+ (Stene *et al.*, 2020)}, and in $[W_2O_4F_6]^{2-}$ (Wollert *et al.*, 1991).

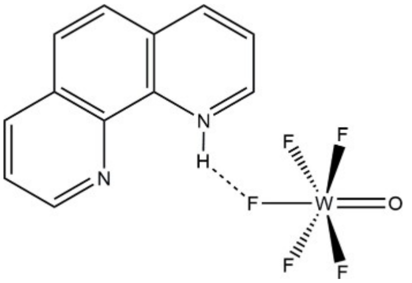

Crystallographically characterized $[WOF_5]^-$ salts with a range of counterions {$[As(C_6H_5)_4]^+$ (Massa *et al.*, 1982); $[Cs(15\text{-crown-}5)_2]^+$ (Nuszhär *et al.*, 1992); Ag^{2+} (Mazej *et al.*, 2017); $[WF_4(1,2\text{-}\{P(CH_3)_2\}_2C_6H_4)]^{2+}$ (Levason *et al.*, 2018)} have exhibited some degree of O/F disorder in the anion, obfuscating the W=O and W—F bond lengths. Recently, however, $[Xe_2F_{11}][WOF_5]$ and $[XeF_5][WOF_5]\cdot XeOF_4$ were reported to contain $[WOF_5]^-$ anions that are ordered as a consequence of multiple Xe···F—W interactions (Bortolus *et al.*, 2020). Herein, we report a new ordered $[WOF_5]^-$ salt in the form of (1,10-phen-H)$[WOF_5]$ (Fig. 1), obtained during an attempted crystallization of WF_6(1,10-phen) (Turnbull *et al.*, 2019*a*).

2. Structural commentary

The W=O bond length in (1,10-phen-H)$[WOF_5]$ [1.698 (2) Å] is indistinguishable from those in $[Xe_2F_{11}][WOF_5]$ [1.698 (3) Å; Bortolus *et al.*, 2020), $WOF_4\{OP(C_6H_5)_3\}$ [1.682 (5) Å; Levason *et al.*, 2016] and $WOF_4(NC_5H_5)$ [1.690 (3) Å; Turnbull *et al.*, 2019*b*]. The $W—F_{eq}$ bond lengths [1.8677 (15)–1.8809 (15) Å] are also insignificantly different from those in $WOF_4\{OP(C_6H_5)_3\}$ [1.857 (3)–1.871 (3) Å; Levason *et al.*, 2016] and $WOF_4(NC_5H_5)$ [1.859 (3)–1.868 (3) Å; Turnbull *et al.*, 2019*b*]. The $W—F_{eq}$ bonds in $[Xe_2F_{11}][WOF_5]$ (Bortolus *et al.*, 2020) are also of similar lengths to those in the title compound, although one terminal $W—F_{eq}$ bond [1.848 (2) Å] is significantly shorter in the $[Xe_2F_{11}]^+$ salt, and one bridging bond significantly longer [1.900 (2) Å].

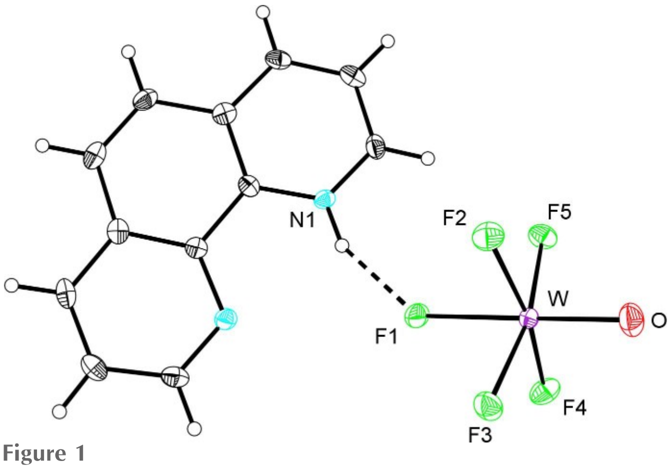

Figure 1
Displacement ellipsoid plot (50% probability level) of (1,10-phen-H)$[WOF_5]$.

Table 1
Bond valences and sums of the $[WOF_5]^-$ anion in (1,10-phen-H)$[WOF_5]$.

	v_i^a		V^b
		W	5.98
W=O	1.81	O	1.88
W—F1	0.62	F1	0.81
W—F2	0.89	F2	0.95
W—F3	0.88	F3	0.94
W—F4	0.90	F4	0.97
W—F5	0.87	F5	0.95

Notes: (*a*) Defined as $v_i = \exp[R_o - R/b]$, where R is the observed bond length (in Å) and R_o and b are empirical parameters (Brown & Altermatt, 1985; Brese & O'Keeffe, 1991; Brown, 2002; Adams *et al.*, 2004). (*b*) Defined as $V = \Sigma(v_i)$. Only secondary contacts within the sum of the van der Waals radii (Bondi, 1964) were considered.

The $W—F_{ax}$ bond length of (1,10-phen-H)$[WOF_5]$ [2.0048 (15) Å] is slightly shorter than those in $[Xe_2F_{11}][WOF_5]$ [2.047 (2) Å; Bortolus *et al.*, 2020] and $[C_5H_5NH][W(NC_6F_5)F_5]$ [2.0212 (13) Å; Turnbull *et al.*, 2017]. In the latter compound, the N1—H1···F1 interaction resulted in significant elongation of the $W—F_{ax}$ bond with respect to that observed in $[N(CH_3)_4][W(NC_6F_5)F_5]$ [1.973 (3) Å; Turnbull *et al.*, 2017]. Gas-phase geometry optimizations of the $[Xe_2F_{11}][WOF_5]$ ion pair and free $[WOF_5]^-$ corroborated a significant elongation of the $W—F_{ax}$ bond in the former anion compared to the latter (2.148 *vs* 1.972 Å, respectively) arising from cation–anion interactions (Bortolus *et al.*, 2020).

The individual bond valences of the $[WOF_5]^-$ anion in (1,10-phen-H)$[WOF_5]$ (Table 1) reveal that the W=O bond ($\nu = 1.81$) is approximately double the strength of the $W—F_{eq}$ bonds ($\nu = 0.87$–0.90), indicating complete O/F ordering; in a disordered anion, the W=O bond valence is artificially decreased due to averaging with the W—F single bonds. The F1 atom possesses a valence sum significantly less than unity ($V = 0.81$) because of the *trans* influence of the oxido ligand and N1—H1···F1 hydrogen-bonding interaction substantially polarizing that bond.

3. Supramolecular features

Besides the N1—H1···F1 hydrogen-bonding interactions, there also exist weak intermolecular C5···O [3.163 (3) Å] and C3···C10 [3.204 (4) Å] interactions that result in the formation of columns of cations and anions running parallel to the *a* axis (Fig. 2) in the packed crystal. The crystal packing, however, appears to be dominated by the N1—H1···F1 hydrogen bonds (Table 2) and other intermolecular interactions, such as π–π stacking interactions between cations, are absent.

Table 2
Hydrogen-bond geometry (Å, °).

D—H$\cdots$$A$	D—H	H$\cdots$$A$	$D\cdots A$	D—H$\cdots$$A$
N1—H1$\cdots$F1	0.89 (3)	1.88 (3)	2.704 (3)	154 (3)

4. Synthesis and crystallization

In the dry box, a 1/4"-o.d. FEP reactor, equipped with a 316-stainless-steel valve and pre-passivated with F_2 (100%, Linde Gas), was charged with WF_6(1,10-phen) (*ca* 0.01 g), prepared as described previously (Turnbull *et al.*, 2019*a*). Acetonitrile (*ca* 0.1 mL), dried as previously described (Winfield, 1984), was distilled into the reactor through a glass vacuum line equipped with grease-free PTFE stopcocks (J. Young). The reactor was heated to 353 K in a hot-water bath and allowed to cool to ambient temperature over 16 h. The reactor was then cooled rapidly to 233 K and the solvent was removed under dynamic vacuum at that temperature, resulting in the formation of colourless needles of (1,10-phen-H)[WOF_5], together with an off-white microcrystalline material that was not further characterized, but is presumed to contain WF_6(1,10-phen) and (1,10-phen-H)[WOF_5].

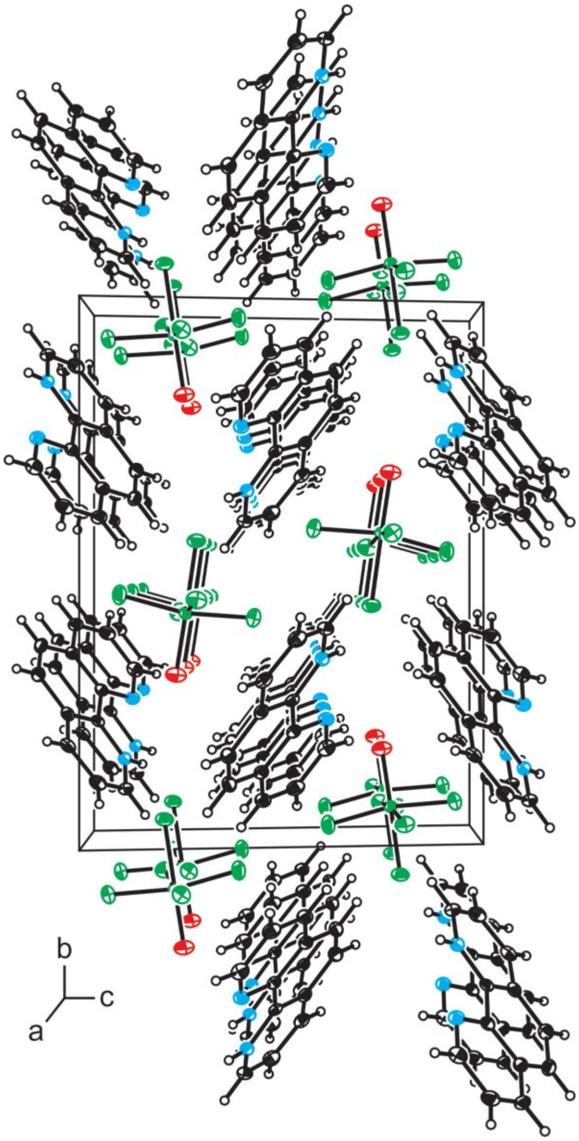

Figure 2
Crystal packing of (1,10-phen-H)[WOF_5] viewed along the *a* axis.

Table 3
Experimental details.

Crystal data	
Chemical formula	$(C_{12}H_9N_2)[WOF_5]$
M_r	476.06
Crystal system, space group	Monoclinic, $P2_1/n$
Temperature (K)	112
a, b, c (Å)	7.1664 (2), 15.5088 (4), 11.6516 (4)
β (°)	101.202 (3)
V (Å^3)	1270.31 (7)
Z	4
Radiation type	Mo $K\alpha$
μ (mm^{-1})	9.16
Crystal size (mm)	0.27 × 0.12 × 0.06
Data collection	
Diffractometer	Rigaku SuperNova, Dual source (Mo and Cu), Pilatus 200/300K
Absorption correction	Analytical [numerical absorption correction using a multifaceted crystal model based on expressions derived by Clark & Reid (1995) implemented in *CrysAlis PRO* (Rigaku OD, 2015). Empirical absorption correction using spherical harmonics, implemented in SCALE3 ABSPACK]
$T_{\min}$, $T_{\max}$	0.447, 0.645
No. of measured, independent and observed [$I > 2\sigma(I)$] reflections	15835, 2908, 2652
R_{int}	0.033
$(\sin \theta/\lambda)_{\max}$ (Å^{-1})	0.649
Refinement	
$R[F^2 > 2\sigma(F^2)]$, $wR(F^2)$, S	0.016, 0.038, 1.06
No. of reflections	2908
No. of parameters	194
H-atom treatment	H atoms treated by a mixture of independent and constrained refinement
$\Delta\rho_{\max}$, $\Delta\rho_{\min}$ (e Å^{-3})	0.97, −0.83

Computer programs: *CrysAlis PRO* (Rigaku OD, 2015), *SHELXT* (Sheldrick, 2015*a*), *SHELXL* (Sheldrick, 2015*b*), *XP* (Sheldrick, 2008), *OLEX2* (Dolomanov *et al.*, 2009) and *publCIF* (Westrip, 2010).

The reactor was cut open and the crystals transferred onto an aluminium trough cooled to 193 K under a constant stream of liquid-N_2-cooled, dry N_2. The selected crystal was affixed to a Nylon cryo-loop submerged in perfluorinated polyether oil (Fomblin Z-25) and quickly transferred to the goniometer to minimize exposure to air.

5. Refinement details

Crystallographic data collection and refinement parameters are summarized in Table 3. All the hydrogen atoms were located in difference Fourier maps and were refined using a riding model, with the exception of H1, the position of which was refined freely (Table 2).

Acknowledgements

We thank the Natural Sciences and Engineering Research Council of Canada (NSERC) for awarding a Discovery grant to MG as well as CGS-M and PGS-D scholarships to DT. In addition, we would like to thank the University of Lethbridge for awarding the SGS Dean's Scholarship and Tuition Award to DT and supporting this work.

Funding information

Funding for this research was provided by: Natural Sciences and Engineering Research Council of Canada (grant No. 261340-2013 to Michael Gerken; scholarship to Douglas Turnbull).

References

Abrahams, S. C., Marsh, P. & Ravez, J. (1987). *J. Chem. Phys.* **87**, 6012–6020.
Adams, S., Moretzki, O. & Canadell, E. (2004). *Solid State Ionics*, **168**, 281–290.
Arnaudet, L., Bougon, R., Ban, B., Lance, M., Navaza, A., Nierlich, M. & Vigner, J. (1992). *J. Fluorine Chem.* **59**, 141–152.
Asprey, L. B., Ryan, R. R. & Fukushima, E. (1972). *Inorg. Chem.* **11**, 3122–3122.
Bennett, M. J., Haas, T. E. & Purdham, J. T. (1972). *Inorg. Chem.* **11**, 207–208.
Bondi, A. (1964). *J. Phys. Chem.* **68**, 441–451.
Bortolus, M. R., Mercier, H. P. A. & Schrobilgen, G. J. (2020). *Chem. Eur. J.* **26**, 8935–8950.
Brese, N. E. & O'Keeffe, M. (1991). *Acta Cryst.* B**47**, 192–197.
Brown, I. D. (2002). *The Chemical Bond in Inorganic Chemistry: The Bond Valence Model*. Oxford University Press.
Brown, I. D. & Altermatt, D. (1985). *Acta Cryst.* B**41**, 244–247.
Chaminade, J. P., Moutou, J. M., Villeneuve, G., Couzi, M., Pouchard, M. & Hagenmuller, P. (1986). *J. Solid State Chem.* **65**, 27–39.
Clark, R. C. & Reid, J. S. (1995). *Acta Cryst.* A**51**, 887–897.
Crossman, M. C., Fawcett, J., Hope, E. G. & Russell, D. R. (1996). *J. Organomet. Chem.* **514**, 87–91.
Dolomanov, O. V., Bourhis, L. J., Gildea, R. J., Howard, J. A. K. & Puschmann, H. (2009). *J. Appl. Cryst.* **42**, 339–341.
Edwards, A. J. & Jones, G. R. (1968). *J. Chem. Soc. A*, pp. 2074–2078.
Hoskins, B. F., Linden, A. & O'Donnell, T. A. (1987). *Inorg. Chem.* **26**, 2223–2228.
Levason, W., Monzittu, F. M., Reid, G. & Zhang, W. (2018). *Chem. Commun.* **54**, 11681–11684.
Levason, W., Reid, G. & Zhang, W. (2016). *J. Fluorine Chem.* **184**, 50–57.
Massa, W., Hermann, S. & Dehnicke, K. (1982). *Z. Anorg. Allg. Chem.* **493**, 33–40.
Mazej, Z., Gilewski, T., Goreshnik, E. A., Jagličić, Z., Derzsi, M. & Grochala, W. (2017). *Inorg. Chem.* **56**, 224–233.
Nuszhär, D., Weller, F., Dehnicke, K. & Hiller, W. (1992). *J. Alloys Compd.* **183**, 30–44.
Rigaku OD (2015). *CrysAlis PRO*. Rigaku Oxford Diffraction, Oxford, England.
Sheldrick, G. M. (2008). *Acta Cryst.* A**64**, 112–122.
Sheldrick, G. M. (2015*a*). *Acta Cryst.* A**71**, 3–8.
Sheldrick, G. M. (2015*b*). *Acta Cryst.* C**71**, 3–8.
Srivastava, A. M. & Ackerman, J. F. (1992). *J. Solid State Chem.* **98**, 144–150.
Stene, R., Scheibe, B., Karttunen, A. J., Petry, W. & Kraus, F. (2020). *Eur. J. Inorg. Chem.* pp. 2260–2269.
Turnbull, D., Wetmore, S. D. & Gerken, M. (2017). *Inorg. Chem.* **56**, 12581–12593.
Turnbull, D., Wetmore, S. D. & Gerken, M. (2019*a*). *Angew. Chem. Int. Ed.* **58**, 13035–13038.
Turnbull, D., Wetmore, S. D. & Gerken, M. (2019*b*). *Inorg. Chem.* **58**, 6363–6375.
Udovenko, A. A. & Laptash, N. M. (2008*a*). *Acta Cryst.* B**64**, 645–651.
Udovenko, A. A. & Laptash, N. M. (2008*b*). *Acta Cryst.* B**64**, 305–311.
Vlasse, M., Moutou, J., Cervera-Marzal, M., Chaminade, J. & Hagenmuller, P. (1982). *Rev. Chim. Miner.* **19**, 58–64.
Voit, E. I., Voit, A. V., Mashkovskii, A. A., Laptash, N. M. & Kavun, V. Y. (2006). *J. Struct. Chem.* **47**, 642–650.
Welk, M. E., Norquist, A. J., Stern, C. L. & Poeppelmeier, K. R. (2001). *Inorg. Chem.* **40**, 5479–5480.
Westrip, S. P. (2010). *J. Appl. Cryst.* **43**, 920–925.
Winfield, J. M. (1984). *J. Fluor. Chem.* **25**, 91–98.
Wollert, R., Rentschler, E., Massa, W. & Dehnicke, K. (1991). *Z. Anorg. Allg. Chem.* **596**, 121–132.

supporting information

Acta Cryst. (2020). E**76**, 1345-1348   [https://doi.org/10.1107/S2056989020009767]

Crystal structure of an ordered $[WOF_5]^-$ salt: (1,10-phen-H)$[WOF_5]$ (1,10-phen = 1,10-phenanthroline)

Douglas Turnbull and Michael Gerken

Computing details

Data collection: *CrysAlis PRO* 1.171.38.43 (Rigaku OD, 2015); cell refinement: *CrysAlis PRO* (Rigaku OD, 2015); data reduction: *CrysAlis PRO* 1.171.38.43 (Rigaku OD, 2015); program(s) used to solve structure: ShelXT (Sheldrick, 2015a); program(s) used to refine structure: *SHELXL* (Sheldrick, 2015b); molecular graphics: *XP* (Sheldrick, 2008); software used to prepare material for publication: *OLEX2* (Dolomanov *et al.*, 2009) and *publCIF* (Westrip, 2010).

1,10-Phenanthrolinium pentafluoridooxidotungstate(VI)

Crystal data

$(C_{12}H_9N_2)[WOF_5]$
$M_r = 476.06$
Monoclinic, $P2_1/n$
$a = 7.1664$ (2) Å
$b = 15.5088$ (4) Å
$c = 11.6516$ (4) Å
$\beta = 101.202$ (3)°
$V = 1270.31$ (7) Å^3
$Z = 4$
$F(000) = 888$
$D_x = 2.489$ Mg m^{-3}
Mo $K\alpha$ radiation, $\lambda = 0.71073$ Å
Cell parameters from 8493 reflections
$\theta = 3.6$–31.4°
$\mu = 9.15$ mm^{-1}
$T = 112$ K
Needle, clear colourless
0.27 × 0.12 × 0.06 mm

Data collection

Rigaku SuperNova, Dual source (Mo and Cu), Pilatus 200/300K diffractometer
Radiation source: micro-focus sealed X-ray tube, SuperNova (Mo) X-ray Source
Mirror monochromator
ω scans
Absorption correction: analytical [Numeric absorption correction using a multifaceted crystal model based on expressions derived by Clark & Reid (1995) implemented in CrysAlisPro (Rigaku OD, 2015). Empirical absorption correction using spherical harmonics, implemented in SCALE3 ABSPACK]
$T_{min} = 0.447$, $T_{max} = 0.645$
15835 measured reflections
2908 independent reflections
2652 reflections with $I > 2\sigma(I)$
$R_{int} = 0.033$
$\theta_{max} = 27.5°$, $\theta_{min} = 3.4°$
$h = -9 \rightarrow 9$
$k = -19 \rightarrow 20$
$l = -15 \rightarrow 13$

Refinement

Refinement on F^2	Hydrogen site location: mixed
Least-squares matrix: full	H atoms treated by a mixture of independent and constrained refinement
$R[F^2 > 2\sigma(F^2)] = 0.016$	$w = 1/[\sigma^2(F_o^2) + (0.0179P)^2 + 0.7231P]$ where $P = (F_o^2 + 2F_c^2)/3$
$wR(F^2) = 0.038$	$(\Delta/\sigma)_{max} = 0.002$
$S = 1.06$	$\Delta\rho_{max} = 0.97$ e Å^{-3}
2908 reflections	$\Delta\rho_{min} = -0.83$ e Å^{-3}
194 parameters	
0 restraints	
Primary atom site location: dual	

Special details

Geometry. All esds (except the esd in the dihedral angle between two l.s. planes) are estimated using the full covariance matrix. The cell esds are taken into account individually in the estimation of esds in distances, angles and torsion angles; correlations between esds in cell parameters are only used when they are defined by crystal symmetry. An approximate (isotropic) treatment of cell esds is used for estimating esds involving l.s. planes.

Fractional atomic coordinates and isotropic or equivalent isotropic displacement parameters (Å^2)

	x	y	z	$U_{iso}*/U_{eq}$
W1	0.45262 (2)	0.57004 (2)	0.26707 (2)	0.01171 (4)
F1	0.4234 (2)	0.44319 (10)	0.29168 (15)	0.0209 (3)
F2	0.4618 (2)	0.57848 (10)	0.42837 (14)	0.0226 (4)
F3	0.7145 (2)	0.54615 (11)	0.29703 (15)	0.0222 (3)
F4	0.4359 (2)	0.53785 (11)	0.11094 (13)	0.0233 (3)
F5	0.1857 (2)	0.56900 (10)	0.24578 (15)	0.0202 (3)
O1	0.4729 (3)	0.67755 (13)	0.24458 (18)	0.0242 (4)
N1	0.1998 (3)	0.35275 (14)	0.41042 (18)	0.0134 (4)
H1	0.286 (4)	0.3659 (19)	0.368 (2)	0.014 (7)*
N2	0.4933 (3)	0.24312 (14)	0.39891 (19)	0.0154 (4)
C1	0.0520 (4)	0.40604 (17)	0.4040 (2)	0.0172 (5)
H1A	0.041718	0.455156	0.354409	0.021*
C2	−0.0870 (4)	0.39002 (18)	0.4694 (2)	0.0198 (6)
H2	−0.195569	0.426242	0.462155	0.024*
C3	−0.0649 (4)	0.32076 (17)	0.5449 (2)	0.0170 (5)
H3	−0.156152	0.310602	0.592588	0.020*
C4	0.0917 (4)	0.26498 (17)	0.5518 (2)	0.0151 (5)
C5	0.2231 (3)	0.28172 (16)	0.4800 (2)	0.0129 (5)
C6	0.3802 (3)	0.22474 (16)	0.4765 (2)	0.0133 (5)
C7	0.4049 (3)	0.15380 (17)	0.5530 (2)	0.0153 (5)
C8	0.5628 (4)	0.10033 (18)	0.5500 (2)	0.0189 (5)
H8	0.588937	0.052531	0.601602	0.023*
C9	0.6790 (4)	0.11795 (18)	0.4715 (2)	0.0204 (6)
H9	0.785780	0.082457	0.467828	0.024*
C10	0.6365 (4)	0.18924 (17)	0.3973 (2)	0.0190 (5)
H10	0.715470	0.199719	0.342053	0.023*
C11	0.1198 (4)	0.19063 (17)	0.6274 (2)	0.0181 (5)
H11	0.032761	0.178632	0.677319	0.022*
C12	0.2702 (4)	0.13793 (18)	0.6272 (2)	0.0187 (5)
H12	0.287124	0.089145	0.677491	0.022*

Atomic displacement parameters (Å²)

	U^{11}	U^{22}	U^{33}	U^{12}	U^{13}	U^{23}
W1	0.01223 (6)	0.01049 (6)	0.01259 (6)	−0.00060 (3)	0.00287 (4)	0.00057 (4)
F1	0.0272 (8)	0.0131 (8)	0.0256 (8)	−0.0023 (6)	0.0129 (7)	−0.0004 (6)
F2	0.0277 (9)	0.0254 (9)	0.0147 (8)	−0.0001 (7)	0.0044 (7)	−0.0030 (6)
F3	0.0153 (8)	0.0213 (8)	0.0298 (9)	0.0018 (6)	0.0037 (7)	0.0017 (7)
F4	0.0282 (9)	0.0284 (9)	0.0145 (7)	−0.0049 (7)	0.0071 (6)	−0.0014 (7)
F5	0.0121 (7)	0.0233 (9)	0.0249 (8)	0.0003 (6)	0.0027 (6)	−0.0025 (6)
O1	0.0249 (10)	0.0152 (10)	0.0320 (11)	−0.0003 (8)	0.0043 (9)	0.0021 (8)
N1	0.0137 (10)	0.0133 (10)	0.0140 (10)	−0.0023 (8)	0.0051 (9)	−0.0005 (8)
N2	0.0162 (10)	0.0131 (11)	0.0179 (11)	−0.0016 (8)	0.0058 (9)	0.0000 (9)
C1	0.0209 (13)	0.0119 (12)	0.0185 (13)	0.0018 (10)	0.0029 (11)	0.0012 (10)
C2	0.0179 (13)	0.0183 (14)	0.0238 (14)	0.0031 (11)	0.0056 (11)	−0.0047 (11)
C3	0.0167 (12)	0.0166 (12)	0.0191 (13)	−0.0019 (10)	0.0065 (10)	−0.0060 (10)
C4	0.0151 (12)	0.0154 (13)	0.0143 (12)	−0.0044 (10)	0.0017 (10)	−0.0038 (10)
C5	0.0131 (11)	0.0107 (12)	0.0142 (11)	−0.0015 (9)	0.0007 (9)	−0.0036 (10)
C6	0.0127 (11)	0.0126 (12)	0.0143 (11)	−0.0022 (9)	0.0018 (9)	−0.0027 (9)
C7	0.0158 (12)	0.0133 (12)	0.0151 (12)	−0.0025 (10)	−0.0011 (10)	−0.0013 (10)
C8	0.0210 (13)	0.0139 (12)	0.0189 (13)	0.0024 (11)	−0.0035 (11)	0.0010 (11)
C9	0.0185 (13)	0.0168 (14)	0.0250 (14)	0.0034 (10)	0.0023 (11)	−0.0042 (11)
C10	0.0152 (12)	0.0200 (14)	0.0231 (13)	−0.0010 (10)	0.0072 (11)	−0.0036 (11)
C11	0.0220 (13)	0.0174 (13)	0.0167 (12)	−0.0040 (10)	0.0083 (11)	−0.0001 (10)
C12	0.0232 (13)	0.0176 (13)	0.0143 (12)	−0.0047 (11)	0.0008 (10)	0.0018 (10)

Geometric parameters (Å, º)

W1—F1	2.0048 (15)	C3—C4	1.407 (4)
W1—F2	1.8724 (16)	C4—C5	1.400 (4)
W1—F3	1.8779 (15)	C4—C11	1.441 (4)
W1—F4	1.8677 (15)	C5—C6	1.438 (4)
W1—F5	1.8809 (15)	C6—C7	1.405 (4)
W1—O1	1.698 (2)	C7—C8	1.409 (4)
N1—H1	0.89 (3)	C7—C12	1.437 (4)
N1—C1	1.334 (3)	C8—H8	0.9500
N1—C5	1.359 (3)	C8—C9	1.379 (4)
N2—C6	1.357 (3)	C9—H9	0.9500
N2—C10	1.326 (3)	C9—C10	1.400 (4)
C1—H1A	0.9500	C10—H10	0.9500
C1—C2	1.389 (4)	C11—H11	0.9500
C2—H2	0.9500	C11—C12	1.353 (4)
C2—C3	1.378 (4)	C12—H12	0.9500
C3—H3	0.9500		
F2—W1—F1	84.80 (7)	C3—C4—C11	122.8 (2)
F2—W1—F3	89.33 (7)	C5—C4—C3	118.3 (2)
F2—W1—F5	88.24 (7)	C5—C4—C11	118.9 (2)
F3—W1—F1	84.73 (7)	N1—C5—C4	119.2 (2)

F3—W1—F5	167.69 (7)	N1—C5—C6	119.2 (2)
F4—W1—F1	83.59 (7)	C4—C5—C6	121.6 (2)
F4—W1—F2	168.37 (7)	N2—C6—C5	117.5 (2)
F4—W1—F3	90.06 (7)	N2—C6—C7	124.7 (2)
F4—W1—F5	89.89 (7)	C7—C6—C5	117.7 (2)
F5—W1—F1	83.04 (7)	C6—C7—C8	116.6 (2)
O1—W1—F1	178.86 (8)	C6—C7—C12	120.0 (2)
O1—W1—F2	95.67 (8)	C8—C7—C12	123.5 (2)
O1—W1—F3	96.31 (8)	C7—C8—H8	120.3
O1—W1—F4	95.93 (9)	C9—C8—C7	119.5 (2)
O1—W1—F5	95.94 (8)	C9—C8—H8	120.3
C1—N1—H1	117.1 (19)	C8—C9—H9	120.7
C1—N1—C5	122.7 (2)	C8—C9—C10	118.6 (2)
C5—N1—H1	120.1 (19)	C10—C9—H9	120.7
C10—N2—C6	116.2 (2)	N2—C10—C9	124.4 (2)
N1—C1—H1A	119.9	N2—C10—H10	117.8
N1—C1—C2	120.3 (2)	C9—C10—H10	117.8
C2—C1—H1A	119.9	C4—C11—H11	120.0
C1—C2—H2	120.5	C12—C11—C4	119.9 (2)
C3—C2—C1	119.0 (3)	C12—C11—H11	120.0
C3—C2—H2	120.5	C7—C12—H12	119.1
C2—C3—H3	119.8	C11—C12—C7	121.7 (2)
C2—C3—C4	120.5 (2)	C11—C12—H12	119.1
C4—C3—H3	119.8		

Hydrogen-bond geometry (Å, º)

D—H···*A*	*D*—H	H···*A*	*D*···*A*	*D*—H···*A*
N1—H1···F1	0.89 (3)	1.88 (3)	2.704 (3)	154 (3)